Multimode inversion with amplitude response of surface waves in the spatial autocorrelation method

AUTHOR(S):

Ikeda, Tatsunori; Matsuoka, Toshifumi; Tsuji, Takeshi; Hayashi, Koichi

Geophysical Journal International

Geophys. J. Int. (2012) **190,** 541–552 doi: 10.1111/j.1365-246X.2012.05496.x

Multimode inversion with amplitude response of surface waves in the spatial autocorrelation method

Tatsunori Ikeda,[1] Toshifumi Matsuoka,[1] Takeshi Tsuji[1,*] and Koichi Hayashi[2]

[1]*Department of Urban Management, Kyoto University C1 Kyoto-Daigaku Katsura, Nishikyo-ku, Kyoto-shi, Kyoto* 615-8540, *Japan. E-mail: t_ikeda@earth.kumst.kyoto-u.ac.jp*

[2]*Geometrics,* 2190 *Fortune Drive, San Jose, CA* 95131, *USA*

Accepted 2012 April 4. Received 2012 March 28; in original form 2011 October 12

SUMMARY

Microtremors are usually analysed without any consideration of the higher modes of surface waves. However, recent studies have demonstrated that higher modes contain useful information for improving the inverted *S*-wave velocity model. In this study, we propose two inversion methods that consider higher modes by using the amplitude response of each mode, which can avoid mode misidentification in the spatial autocorrelation (SPAC) method. One method is to compare the observed phase velocities by the extended spatial autocorrelation (ESPAC) method with the effective phase velocities calculated from theoretical dispersion curves and the amplitude responses of each mode. In the other method, SPAC coefficients are fit directly by comparing theoretical SPAC coefficients determined from dispersion curves and amplitude responses with the observed ones. The latter, direct-fitting approach is much simpler than the method using effective phase velocities. To investigate the effectiveness of these methods, a simulation study was conducted. Simulated microtremors that included higher modes were successfully inverted by the proposed multimode methods. The observed phase velocities and SPAC coefficients determined from field data were also consistent with theoretical ones constructed by the proposed methods except at low frequencies. The inversion using effective phase velocities required prior information about an infinite half-space to obtain a better *S*-wave velocity model whereas the direct-fitting inversion worked well without prior information, suggesting the direct-fitting method is more robust than the method using effective phase velocities. We conclude that our proposed inversion methods are effective for estimating the *S*-wave velocity structure even if higher modes of surface waves are predominant in observed microtremors.

Key words: Surface waves and free oscillations; Statistical seismology; Wave propagation.

GJI Seismology

1 INTRODUCTION

The microtremor method (Okada 2003) has been applied to the estimation of *S*-wave velocity structures by using surface waves (e.g. Okada 2003; Bonnefoy-Claudet *et al.* 2006b). The method has been used mainly for geotechnical site characterization (e.g. Tokimatsu 1997; Roberts & Asten 2004; Richwalski *et al.* 2007). Because the method is non-destructive and needs no active sources, it is inexpensive and easy to apply in various environments. The spatial autocorrelation (SPAC) method (Aki 1957,1965) and the frequency–wavenumber (F–K) method (Capon 1969) are the two main approaches for estimating the dispersion curves of surface waves from microtremor data. Recently, Cho *et al.* (2004, 2006) developed the centreless circular array (CCA) method which uses a miniature circular array. Analysis using refraction microtremors (ReMi; Louie 2001) and time domain analysis (Chávez-García & Luzón 2005) has also been proposed. In this paper, we focus on the SPAC method, whose effectiveness has been demonstrated at various sites, and discuss how to perform a stable inversion with higher modes of surface waves included in microtremors.

The SPAC method can extract the phase velocities of surface waves from microtremor array observations. The *S*-wave velocity structure is then estimated from an inversion of the phase velocities. Surface waves have different modes of propagation. The mode which has lowest velocity is called fundamental mode, whereas the modes which propagate faster than the fundamental mode are called higher modes. Higher modes play an important role if a stiff layer overlies a soft layer or is embedded in soft layers (Gucunski & Woods 1992; Tokimatsu *et al.* 1992a). Xia *et al.* (2003) showed that consideration of higher modes improves the resolution of the inversion and makes its sensitivity deep. However,

*Now at: International Institute for Carbon-Neutral Energy Research (WPI-12CNER), Kyushu Universitv. Motooka. Nishi-Ku, Fukuoka 819-0395, Japan.

observed microtremors have been analysed on the assumption that the fundamental component is predominant in the SPAC method, though some studies have shown that the effect of higher modes included in microtremors is not negligible (e.g. Tokimatsu 1997; Ohori *et al* 2002; Fotti 2005; Feng *et al.* 2005; Asten & Robert 2006). If higher modes of surface waves are predominant in the observed microtremors, analysis without any considerations of higher modes would make it difficult to determine a unique velocity model. Thus, a method that considers higher modes in the SPAC method is required.

Aki (1957) proposed an implementation of the SPAC method when a wave is composed of partial waves with different phase velocities. The proposal regards observed spatial autocorrelation (SPAC) coefficients as a superposition of each mode component weighted by its power fraction. By applying this idea to higher modes, several multi-mode analysis methods in the SPAC method have been proposed. Asten (1976, 2001) proposed an analysis method that separates each mode component by solving the phase velocities and energy fractions of the two modes from the observed data. Asten *et al.* (2004) and Asten & Robert (2006) also proposed a method to recognize higher modes in direct-fitting method of SPAC coefficients (Asten *et al.* 2002, 2004), which is called multimode SPAC (MMSPAC). Asten & Robert (2006) demonstrated the effectiveness of MMSPAC, though they failed to identify higher mode propagation in a simulated data analysis.

Another multimode analysis method was proposed by Tokimatsu *et al.* (1992a,b) and Tokimatsu (1997). If the phase velocities of each mode cannot be separated, the observed phase velocities may not be explained by only one mode. These velocities are called apparent or effective velocities (Socco *et al.* 2010) or fallacious estimates of phase velocities (Yokoi 2010). The approach is to evaluate numerically the theoretical effective phase velocities corresponding to the observed ones by using the energy fractions of each mode from the amplitude response (Harkrider 1964, 1970) using a given subsurface model. For inversion, this evaluated effective phase velocities are compared with corresponding to the observed phase velocities. This multimode method is superior to the former one in that the phase velocities and energy fractions of each mode do not have to be extracted from the observed microtremors, which makes it easier to increase the number of modes in an inversion. Furthermore, this advantage contributes to the avoidance of mode misidentification, which sometimes causes notable error in the results (e.g. Zhang & Chan 2003; O'Neill & Matsuoka 2005). Ohori *et al.* (2002) and Obuchi *et al.* (2004) applied this approach to the SPAC method and performed a successful analysis. In addition, Yokoi (2010) derived the power partition ratio of each mode in the SPAC and CCA methods by using the theory of seismic interferometry, and showed better inversion performance with dual-mode inversion than with single mode.

When higher modes are considered, the effective phase velocities are functions of the receiver separation distance in addition to the frequency, whereas the phase velocities of each mode are functions only of the frequency. This implies that the effect of the receiver separation distance has to be considered when applying the extended spatial autocorrelation (ESPAC) method (Ling & Okada 1993; Okada 2003), which is more robust than the SPAC method and determines a phase velocity from the observed SPAC coefficients obtained from all possible pairs of receivers. However, a method for analysing the theoretical effective phase velocities corresponding to the ones estimated by the ESPAC method has not yet been established. Moreover, multimode analysis using amplitude response has not been applied to the direct-fitting method of SPAC coefficients. As we will discuss later, multimode analysis using amplitude response in the direct-fitting method is much simpler than in the ESPAC method.

In this paper, we propose two analysis methods that consider the effect of higher modes and multiple receiver separation distances in the SPAC method using amplitude response. One is to calculate the theoretical effective phase velocities corresponding to the observed phase velocities from the ESPAC method. The other is to compare the observed SPAC coefficients with theoretical ones by a receiver separation distance when considering higher modes. We first simulated microtremors with a model in which higher modes predominate to conduct a quantitative evaluation of the proposed methods. We compared the observed dispersion curve and SPAC coefficients with theoretical ones. Then we estimated *S*-wave velocity models by inversions using the proposed methods. We also apply our methods to field data obtained in Tsukuba City, Japan.

2 THEORY OF THE SPAC METHOD

2.1 Fundamental mode

The basic theory of the SPAC method (Okada 2003; Asten 2006) is summarized as follows. Here we assume that microtremors are mainly composed of surface waves and that the fundamental mode of a surface wave is dominant. If microtremors are observed by a circle array with radius r (Fig. 1), the complex coherencies COH between a central and a circumferential receiver can be defined as

$$\mathrm{COH}(r, \omega, \theta, \phi) = \exp\{\mathrm{i}rk\cos(\theta - \phi)\}, \tag{1}$$

where i is the imaginary number, ω is the angular frequency, k is the wavenumber, θ is the azimuthal angle and ϕ is the azimuth of propagation of a single plane wave across the array. The azimuthal average of θ for the complex coherencies yields SPAC coefficients ρ,

$$\rho(r, \omega) = \frac{1}{2\pi}\int_0^{2\pi} \exp[\mathrm{i}rk\cos(\theta - \phi)]\mathrm{d}\theta = J_0(rk) = J_0\left[\frac{\omega}{c(\omega)}r\right], \tag{2}$$

where J_0 is the Bessel function of the first kind of zero order. The azimuthal average of ϕ for complex coherencies also yields the same result, which indicates that a single pair of receivers is sufficient for plane waves coming from all directions. The phase velocities are estimated by fitting the observed SPAC coefficients to the Bessel function.

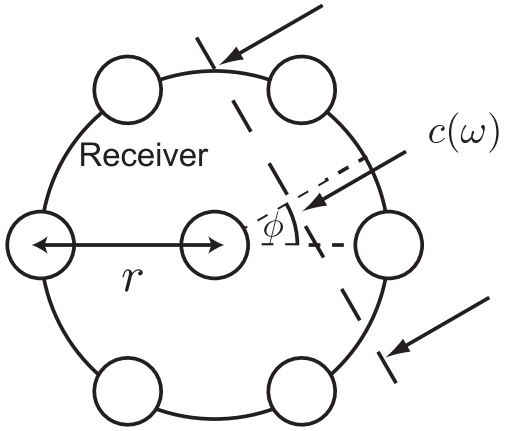

Figure 1. Geometry of a receiver array and an incident plane wave.

2.2 Extended spatial autocorrelation method

If we observe microtremors by using a circular array with radius r_0, SPAC coefficient of angular frequency ω_0 can be written as

$$\rho_{r_0,\omega_0} = J_0\left[\frac{\omega_0}{c(\omega_0)}r_0\right] = J_0(A), \tag{3}$$

where $A = [\frac{\omega_0}{c(\omega_0)}r_0]$ is constant. To estimate a unique phase velocity $c(\omega_0)$, it is necessary to decide upon a unique value of A from the observed SPAC coefficients. However, finding a unique A is difficult, especially near the minima and maxima of the Bessel function.

To overcome this difficulty, Ling & Okada (1993) and Okada (2003) proposed an analysis method called the extended spatial autocorrelation (ESPAC) method. If microtremors are observed by multiple receiver separations, the SPAC coefficient of $\omega = \omega_0$ can be written as

$$\rho_{\omega_0}(r) = J_0\left[\frac{\omega_0}{c(\omega_0)}r\right] = J_0(Br), \tag{4}$$

where $B = [\frac{\omega_0}{c(\omega_0)}]$ is constant. The optimum Bessel function can be found by using the least squares method. To increase the receiver separation distance r, the array observation does not always need to be repeated. As previously mentioned, if we assume that microtremors come from all directions, the observed SPAC coefficients go into the Bessel function without the azimuthal average of θ. Thus, possible pairs of an array can be used in the ESPAC method based on this assumption. Bettig *et al.* (2001) also extended the SPAC method in which arbitrarily shaped arrays can be used by averaging the SPAC coefficients within two circles.

2.3 Multimode analysis

Before we analyse microtremors that include higher modes of surface waves, we have to understand the description of the SPAC coefficients that consider higher modes. The SPAC coefficients that include partial waves with different velocities were derived by Aki (1957) and are defined as

$$\rho(r,\omega) = \sum_i \frac{P_i(\omega)}{P(\omega)} J_0\left[\frac{\omega}{c_i(\omega)}r\right], \tag{5}$$

$$P(\omega) = \sum_i P_i(\omega), \tag{6}$$

where P_i and c_i are the power and the velocity of ith component, respectively. Eq. (5) shows that SPAC coefficients that include partial waves with different velocities can be described as the summation of each component weighted by its power fraction.

Harkrider (1964) derived the relative vertical displacement of the ith Rayleigh mode for a harmonic vertical point force, called the amplitude response (Harkrider 1970). By extending Aki's method to higher modes of surface waves with amplitude response, Tokimatsu *et al.* (1992a) developed the multimode analysis method. Tokimatsu *et al.* (1992a) extracted the mode contribution that depends only on the frequency and regarded the value of its square as the power fraction in eq. (5). It can be written as

$$\frac{P_i(\omega)}{P(\omega)} = \frac{c_i(\omega)A_i^2(\omega)}{\sum_i c_i(\omega)A_i^2(\omega)}, \tag{7}$$

where $A_i(\omega)$ is the amplitude response of ith mode. Note that in Tokimatsu *et al.* (1992a,b) and Tokimatsu (1997) described the Bessel function in eq. (5) by the cosine function, as Tokimatsu *et al.* (1992a,b) and Tokimatsu (1997) applied eq. (7) to F–K analysis on the assumption of 1-D stochastic Rayleigh waves. We assume the power fraction of each mode as eq. (7) in the following discussion. Yokoi (2010) also derived the energy fractions of higher modes from seismic interferometry. The energy fractions by Yokoi (2010) are different from eq. (7).

With this assumption, the theoretical SPAC coefficients (eq. (5)) can be calculated for a horizontally layered medium by using a theoretical dispersion curve and the amplitude response of each mode. In this study, we used DISPER80 (Saito 1988), a computer program that calculates a theoretical dispersion curve and amplitude response. It is clear that if one mode of the surface waves is dominant, the observed phase velocities obtained from the SPAC method correspond to the dominant modes. However, if multimode components are predominant, the observed SPAC coefficients are described by the summation of the Bessel function of each mode weighted by its power fraction. As a result, the observed phase velocities cannot be explained by the theoretical ones of only one mode, and they are called effective (apparent) phase velocities. When considering an inversion analysis, computation of the theoretical effective phase velocities for an assumed layered model is necessary.

Theoretical effective phase velocities can be calculated by the following procedure (Obuchi *et al.* 2004). First, the root mean square error (RMSE) between the Bessel function and the theoretical SPAC coefficients is calculated by the following equation by changing the phase velocity $c(\omega)$:

$$\mathrm{RMSE}(c,\omega) = \sqrt{\left[J_0\left(\frac{\omega}{c(\omega)}r\right) - \sum_i \frac{P_i(\omega)}{P(\omega)} J_0\left(\frac{\omega}{c_i(\omega)}r\right)\right]^2}. \tag{8}$$

Next, the velocity that minimizes RMSE in eq. (8) can be considered to be the theoretical effective phase velocity $c_e(r,\omega)$ at angular frequency ω. These effective phase velocities correspond to the observed ones even if higher modes of surface waves are predominant.

However, it is necessary to modify this method to calculate the effective phase velocities when the ESPAC method is employed. Because the theoretical SPAC coefficients that consider higher modes are no longer described by the Bessel function, the effective phase velocities differ by a receiver separation distance. Ohori *et al.* (2002) compared observed phase velocities estimated from the ESPAC method with effective phase velocities. Ohori *et al.* (2002), however, used only the shortest receiver distance in the calculation of theoretical effective phase velocities. Thus, it is necessary to establish a method to calculate effective phase velocities that gives proper consideration to the receiver separation distances used in the ESPAC method.

Asten *et al.* (2002, 2004) proposed a method of fitting SPAC coefficients directly. In their method, *S*-wave velocity structures are directly inverted by comparing observed SPAC coefficients with theoretical ones. Wathelet *et al.* (2005) estimated *S*-wave velocity profiles from this method by introducing the neighbourhood algorithm. This method has the advantage that there is no need to estimate phase velocities from the observed SPAC coefficients. In spite of its simplicity, the method using the amplitude response has not been applied to the direct-fitting method yet.

Here, we propose two multimode analysis methods that use the amplitude response considering multiple receiver separation distances. One is to calculate theoretical effective phase velocities corresponding to the observed ones obtained by the ESPAC method. The other is to compare the observed SPAC coefficients with theoretical ones using the amplitude response. We will explain details of these methods in the next section.

3 PROPOSED MULTIMODE INVERSION METHODS

3.1 Method using theoretical effective phase velocities

We assume that higher modes are predominant in microtremors data and that the phase velocities are estimated by the ESPAC method. Theoretical effective phase velocities corresponding to the observed ones can be calculated by the following procedure. First, the RMSE between the Bessel function and the theoretical SPAC coefficients are calculated by the following equation by varying the phase velocity $c(\omega)$:

$$\mathrm{RMSE}(c,\omega) = \sqrt{\frac{1}{N}\sum_{j}^{N}\left[J_0\left(\frac{\omega}{c(\omega)}r_j\right) - \sum_i \frac{P_i(\omega)}{P(\omega)} J_0\left(\frac{\omega}{c_i(\omega)}r_j\right)\right]^2}, \quad (9)$$

where r_j is the jth receiver separation distance in an array. Eq. (9) differs from eq. (8) in that the effect of multiple receiver separation distances is evaluated by the summation of the r_j. Next, the velocity that minimizes RMSE in eq. (9) can be considered as the theoretical effective phase velocity $c_e(\omega)$ and corresponds to the observed one from the ESPAC method. If the effective phase velocities calculated from eq. (8) have some differences by a receiver separation distance, eq. (9) would be important to implement a stable inversion in comparison with the method by Ohori *et al.* (2002), which uses the shortest receiver distance in the calculation of theoretical effective phase velocities. The dependence of effective phase velocities with a distance is discussed in appendix. Here, we define the misfit function in an inversion as

$$\mathrm{Misfit} = \sqrt{\frac{1}{M}\sum_{k}^{M}[c_{\mathrm{obs}}(\omega_k) - c_e(\omega_k)]^2}, \quad (10)$$

where c_{obs} is the observed phase velocity obtained by the ESPAC method.

3.2 Method using theoretical SPAC coefficients

If we assume that the observed microtremors dominate the fundamental mode of surface waves, the misfit function in an inversion in the direct-fitting method by Asten *et al.* (2002, 2004) can be defined as

$$\mathrm{Misfit} = \sqrt{\frac{1}{MN}\sum_{k}^{M}\sum_{j}^{N}\left\{\rho_{\mathrm{obs}}(r_j,\omega_k) - J_0\left[\frac{\omega_k}{c(\omega_k)}r_j\right]\right\}^2}, \quad (11)$$

where ρ_{obs} is the observed SPAC coefficient. As Okada (2008) indicated, we can easily introduce their interpretation method to multimodal analysis using amplitude response by eqs (5)–(7). In this case, the misfit function can be defined as

$$\mathrm{Misfit} = \sqrt{\frac{1}{MN}\sum_{k}^{M}\sum_{j}^{N}\left\{\rho_{\mathrm{obs}}(r_j,\omega_k) - \sum_i \frac{P_i(\omega_k)}{P(\omega_k)} J_0\left[\frac{\omega_k}{c_i(\omega_k)}r_j\right]\right\}^2}. \quad (12)$$

3.3 Comparison of the two methods

Fig. 2 shows a flowchart of the multimode analysis methods proposed in the previous section. The left side is for the analysis of

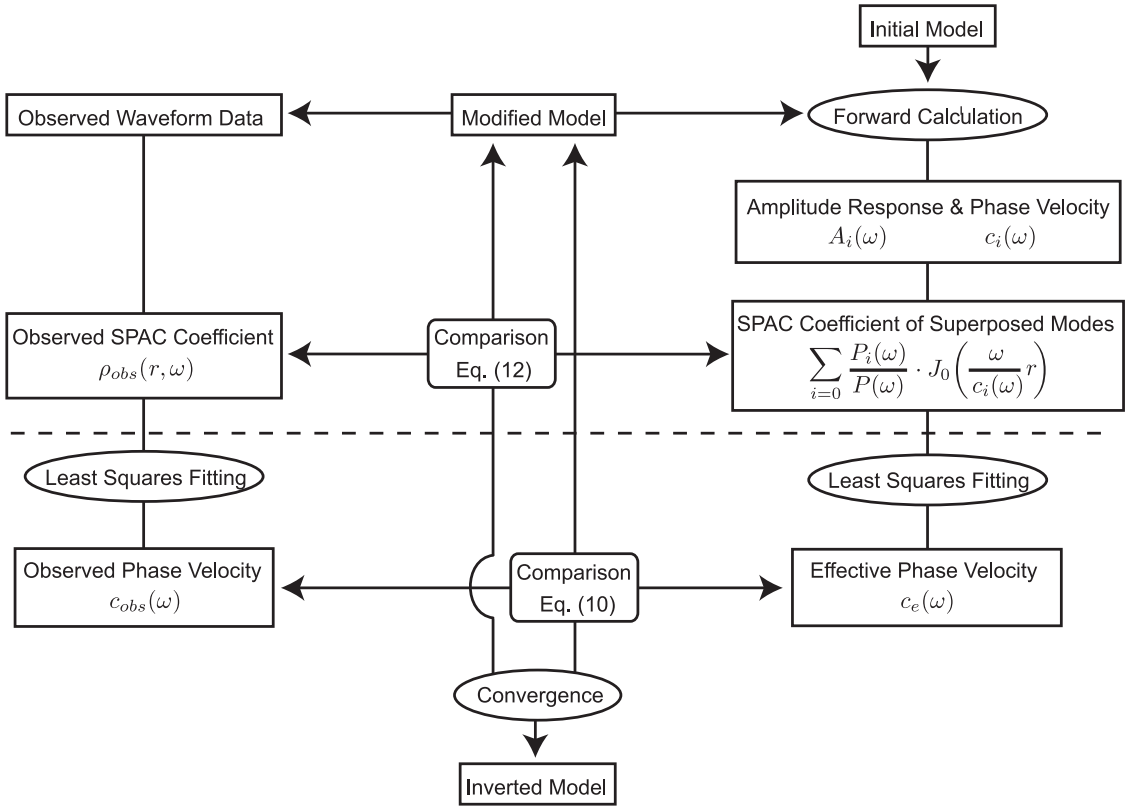

Figure 2. Flowchart of proposed microtremor analyses that consider higher modes and multiple receiver separation distances.

observed data and the right side is for forward modelling of an assumed medium. The final elastic model is decided upon by evaluating the errors between the observed and theoretical values (Fig. 2, central panel). Here, we suppose that the ESPAC method is used in the estimation of the phase velocities. If an analysis method using effective phase velocities is employed, both observed and theoretical (effective) phase velocities will be approximately determined by the least squares fitting. In contrast, the direct-fitting method for comparing SPAC coefficients generates no such estimation errors. Because of this point, the direct-fitting method is superior to the method using effective phase velocities. It should be emphasized that neither proposed method needs to identify the mode of the observed phase velocities and SPAC coefficients.

In the ESPAC method, however, the least squares fitting of observed SPAC coefficients with different receiver separation distances to the Bessel function can reduce errors of the observed SPAC coefficients of each receiver separation distance. In addition, it is beneficial to estimate a dispersion curve even if we analyse microtremors by the direct-fitting of SPAC coefficients. It is known that the *S*-wave velocity structure can be roughly estimated from observed phase velocities by transforming 1.1 times phase velocities versus wavelength/α ($\alpha = 2$–4) to *S*-wave velocities versus depth (e.g. Heisey *et al.* 1982; Abbiss 1983). This *S*-wave velocity structure can be useful to determine an initial model or a search range of model parameters in an inversion if there is no prior information about observation area.

4 SYNTHETIC TEST

To evaluate the effectiveness of the proposed methods, a numerical simulation study was conducted. It is well-known that if the *S*-wave velocity decreases with increasing depth, higher modes of surface waves play a significant role at some frequencies (Gucunski & Woods 1992; Tokimatsu *et al.* 1992a). In the four-layered model used for the simulation study, a high-velocity layer is embedded in low-velocity layers (Fig. 3). Fig. 4 shows the theoretical dispersion curves and power fractions up to the second higher mode. It can be seen that the first higher mode is predominant in the frequency range from 5 to 7.5 Hz. The first higher mode of surface waves would not be negligible in this frequency range. The anomalous predominance of first higher mode can be seen at about 2.5 Hz (Fig. 4b). This anomaly is caused by the appearance of first higher mode with a high amplitude response at a cut-off frequency (Fig. 4a), though the amplitude response of fundamental mode increases in this frequency range. The predominant higher modes in the low-frequency range were studied by Picozzi & Albarello (2007). A similar feature

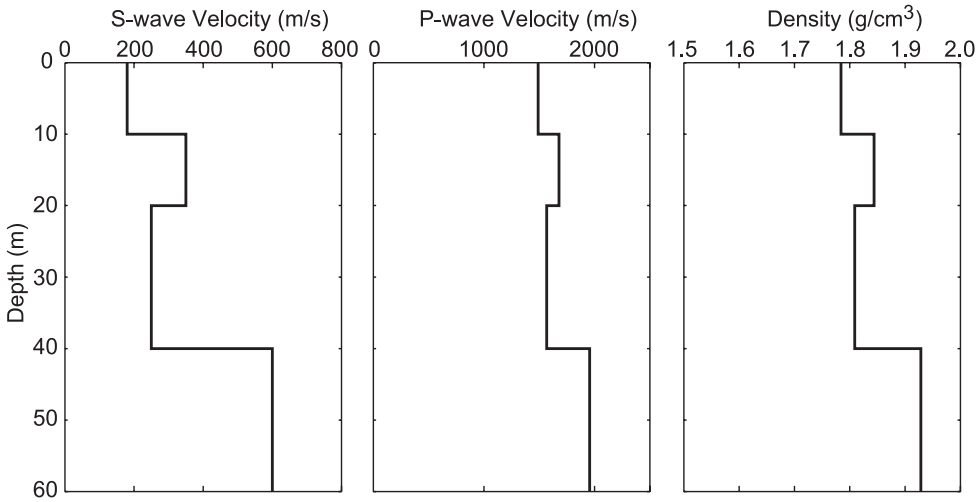

Figure 3. Simulated four-layered model.

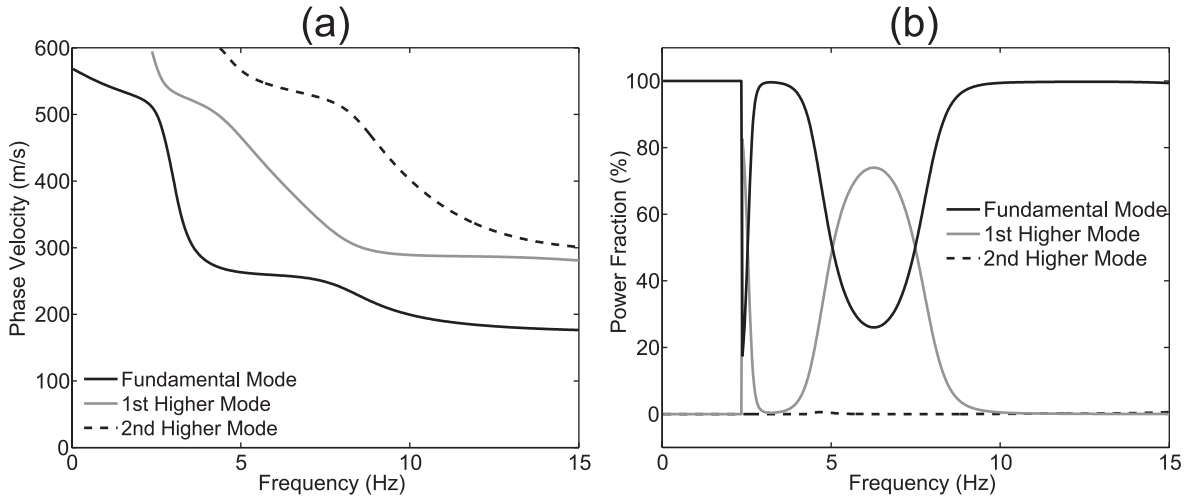

Figure 4. (a) Theoretical dispersion curves and (b) power fractions up to second higher modes for simulated model (Fig. 3).

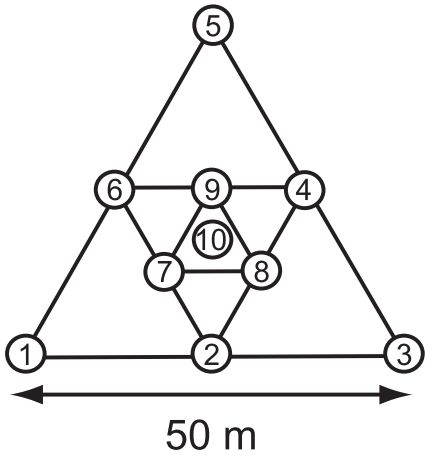

Figure 5. Assumed array shape.

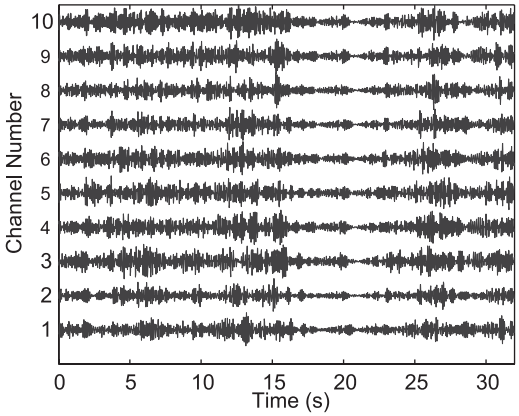

Figure 6. Simulated microtremors from one data set. The receiver number corresponds to Fig. 5.

can be seen in a field example. However, because we mainly use microtremors of the higher frequency range, the predominance of the first higher mode at about 2.5 Hz has little effect on our analysis.

Synthetic microtremors for a 1-D layered model have been successfully simulated by Bonnefoy-Claudet *et al.* (2004, 2006) and Wathelet *et al.* (2005). We simulated microtremors by the following procedure. The Discrete Wavenumber Integral (DWI) method (Bouchon & Aki 1977) was employed for the calculation of waveforms. The source was a vertical force with an 8 Hz Ricker wavelet. For the simplicity, constant and sufficiently large quality factors ($Q = 10\,000$) are given for each layer to ignore anelastic attenuation. A triangular array with 10 receivers (Fig. 5) was assumed in this simulation. One thousand sources were randomly distributed on the surface at radii from 500 to 1000 m from the central receiver of the array and the waveforms were calculated for each source independently. We assume that the wave propagates as a plane wave for the central receiver. Only the vertical component of the waveforms was used to estimate the Rayleigh wave dispersion. Simulated microtremors of about 30 s in duration were synthesized by superposing 50 waveforms randomly chosen from the 1000 waveforms. In this manner, 100 data sets were synthesized. Fig. 6 shows an example of simulated microtremors from one data set.

Next, we applied the proposed methods to the simulated data. The SPAC coefficients were obtained by averaging the azimuthal average of complex coherencies of 100 data sets with a cosine taper in time domain. Fig. 7(a) shows the observed SPAC coefficients for $r = 25$ and 50 m. In addition, the theoretical SPAC coefficients of the superposed modes and theoretical ones up to the first higher mode are shown. The observed SPAC coefficients are in good agreement with the theoretical ones of the superposed modes even if the observed SPAC coefficients are between the fundamental and first higher mode.

By the ESPAC method, the phase velocities were estimated from observed SPAC coefficients of nine different receiver separation distances (Fig. 7(b)). The frequency range of the dispersion curve is determined by the following relation between the wavelength λ and the receiver separation distance r:

$$2r_{\min} < \lambda < 4r_{\max}, \tag{13}$$

where λ is the wavelength of the observed phase velocity, and $r_{\min}$ and $r_{\max}$ are the minimum and maximum receiver separation distance, respectively. The limit of the shortest wavelength is based on the spatial aliasing, whereas the longest one is determined

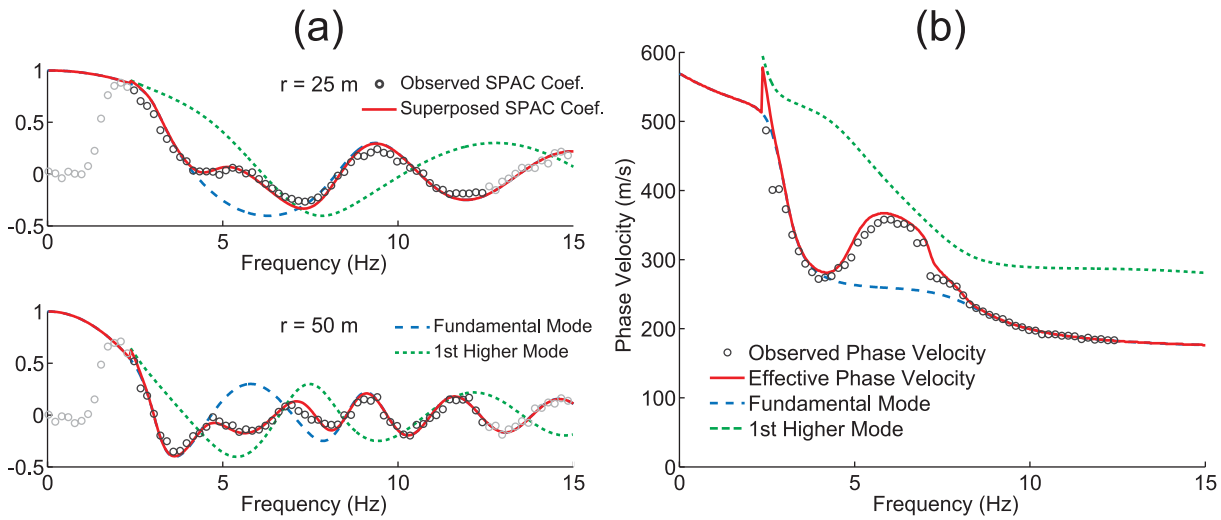

Figure 7. (a) Comparison of the observed SPAC coefficients with theoretical ones (red lines) corresponding to $r = 25$ and 50 m. Only the black circles among the observed SPAC coefficients were used in an inversion. (b) Comparison of the observed phase velocities (black circles) from the ESPAC method with theoretical effective phase velocities (red line).

empirically. The frequency range of SPAC coefficients used in an inversion is the same as that of the estimated phase velocities. Although the observed dispersion curve cannot be separated into dispersion curves for each mode in the frequency range from 5 to 7.5 Hz, the effective phase velocities calculated from eq. (9) are consistent with the observed ones. It can be seen that both proposed methods are effective for multimode analyses that consider multiple receiver separation distances.

S-wave velocity profiles were estimated by inversions in which the proposed methods were introduced into a forward modelling. A genetic algorithm (GA; e.g. Goldberg 1989) with elite selection and dynamic mutation (Yamanaka & Ishida 1996) was employed as the inversion method. The unknown parameters were the *S*-wave velocity and thickness of each layer, as empirical equations (Ludwig *et al.* 1970; Kitsunezaki *et. al*. 1990) were used to obtain the *P*-wave velocity and density from the *S*-wave velocity. The reference *S*-wave velocity model used in the inversion was constructed only from the observed dispersion curve. The depth and *S*-wave velocity (*Vs*) of the reference model are determined by the following wavelength transformation (Heisey *et al.* 1982):

$$\text{Depth} = \frac{1}{3}\lambda_{obs}, \tag{14}$$

$$Vs = 1.1 \times c_{\text{obs}}. \tag{15}$$

A six-layered model was assumed in the inversion. The search range of the *S*-wave velocity and thickness was ±50 per cent for the reference model. The number of generations and the population were 200 and 100, respectively. Twenty trials were performed with the random seeds of an initial population. The final inverted model was constructed by averaging the *S*-wave velocity and thickness for each layer over 20 trials. Theoretical dispersion curves and power fractions were calculated up to the third higher mode in a forward modelling.

Fig. 8 shows the average values of the misfit functions and the standard deviations for each generation. The misfit functions of the last 150 generations show little decrease and the standard derivation of the last generation is quite small, which indicate convergence of the GA inversions. Because objective functions and their dimensions of both methods are different, it is difficult to compare the values of standard deviations. However, standard deviations of the inverted *S*-wave velocity models can be compared because the dimensions of inverted models are same. The *S*-wave velocity profiles estimated from an inversion that introduces two kinds of proposed

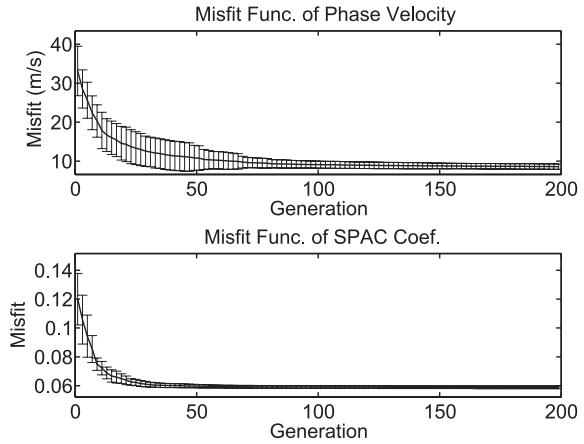

Figure 8. The average of the misfit functions in each generation for simulated data. The error bars show the standard deviations.

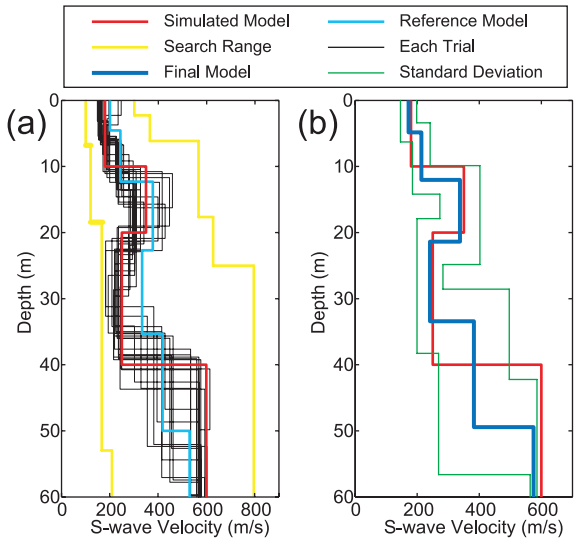

Figure 9. Results of inversions using effective phase velocities. (a) Simulated model (red), reference model constructed by eqs (14) and (15) (cyan), inverted models for each trial (black) and the search range in for the GA inversion (yellow). (b) Final inverted model (blue) obtained by averaging the *S*-wave velocities and thicknesses for each layer over 20 trials and their standard deviations (green).

forward modelling are shown in Figs 9 and 10. The final inverted models and their standard deviations are quite similar. The reversal of the *S*-wave velocity is well-retrieved by either multimode inversion analysis. However, the standard deviations near the infinite half-space are relatively large. This is because the observed phase velocities or SPAC coefficients do not have sufficient sensitivity to deep structure due to a lack of estimated values at lower frequencies.

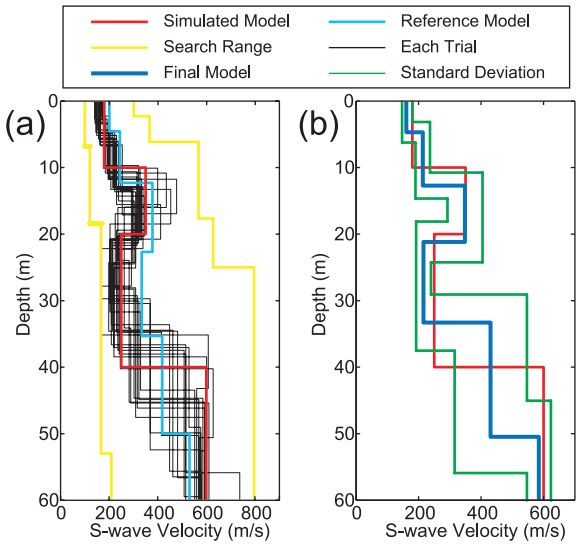

Figure 10. Results of inversions using SPAC coefficients. (a) Simulated model (red), reference model constructed by eqs (14) and (15) (cyan), inverted models for each trial (black) and the search range for the GA inversion (yellow). (b) Final inverted model (blue) obtained by averaging the *S*-wave velocities and thicknesses for each layer over 20 trials and their standard deviations (green).

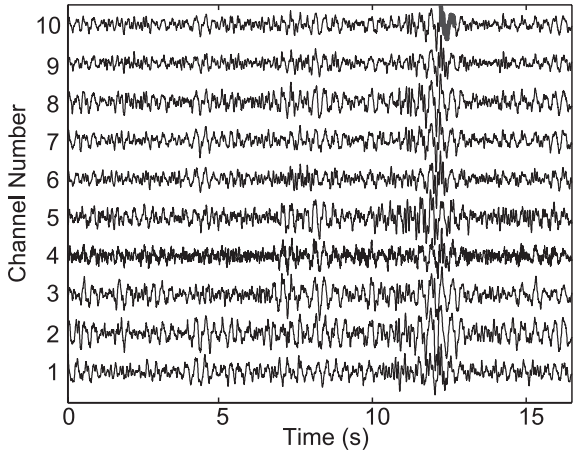

Figure 11. Observed microtremors from one data set. The receiver number corresponds to Fig. 5.

5 FIELD EXAMPLE

We also applied the proposed methods to field data. The survey site is located in Tsukuba City, Japan. Geophones with a natural frequency of 2 Hz were used as receivers. The array shape was similar to that shown in Fig. 5, and the largest aperture of the array was 30 m. The sampling time was 2 ms and each data set consists of 8192 samples. Finally, 300 data sets of about 80 min were obtained. Fig. 11 shows an example of observed microtremors. *P*- and *S*-wave velocities were obtained at this site by PS-logging (Suzuki & Takahashi 1999). Fig. 12 shows the theoretical dispersion curves and power fractions up to the second higher mode constructed from PS-logging data. It can be seen that the power fraction of the first higher mode is predominant near 7.5 Hz. Moreover, the second higher mode has some influence at high frequencies.

The SPAC coefficients and dispersion curve were obtained from 300 data sets in the same way as the synthetic test. Fig. 13(a) shows the observed SPAC coefficients for $r = 15$ and 30 m calculated from

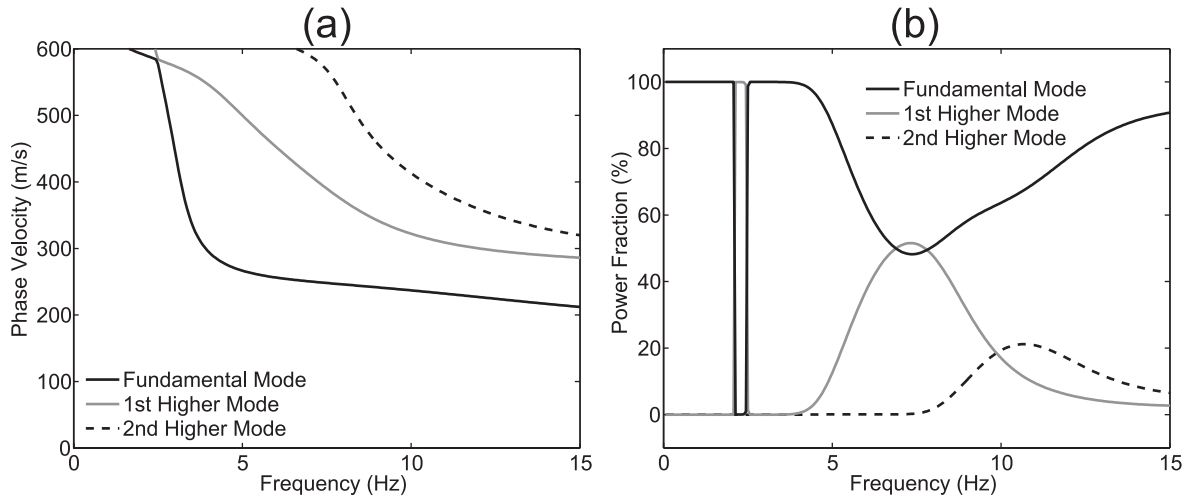

Figure 12. (a) Theoretical dispersion curves and (b) power fractions up to second higher modes for a layered model constructed by PS logging data.

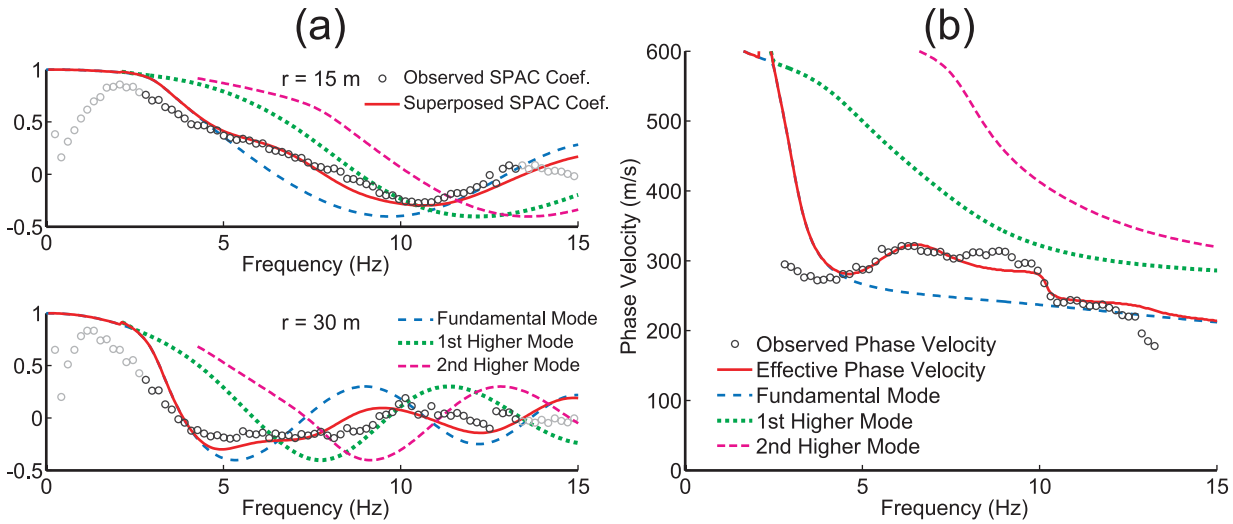

Figure 13. (a) Comparison of observed SPAC coefficients with theoretical ones (red lines) corresponding to $r = 15$ and 30 m. Only the black circles among the observed SPAC coefficients were used in an inversion. (b) Comparison of the observed phase velocities (black circles) from the ESPAC method with theoretical effective phase velocities (red line).

microtremor data. The theoretical SPAC coefficients of the superposed modes and theoretical ones up to the second higher mode are also shown. Fig. 13(b) shows the observed phase velocities from the ESPAC method for which the frequency range was determined by eq. (13). Despite being within this frequency range, phase velocities could not be obtained for frequencies higher than 13.2 Hz because they did not show significant dispersion. In the frequency range from 5 to 10 Hz where the observed SPAC coefficients and phase velocities lie between the fundamental and first higher mode, the observed values are in good agreement with the theoretical ones considering higher modes. However, there are discrepancies between observed and theoretical values below 4 Hz. Fig. 13(a) shows that the observed SPAC coefficient agreed with theoretical one becomes slightly lower with the increase of a receiver separation distance, which indicates these discrepancies depend on the wavelength for a receiver spacing. The phase velocities at lower than 4 Hz are also included in the second and third reliable regions of four regions named as 'acceptable' and 'critical' according to the classification by Cornou *et al.* (2006). Thus, the discrepancies below 4 Hz would be generated from instability of estimated wavelengths.

The *S*-wave velocity profiles were estimated by inversions. The procedure and parameters of the inversions were the same as in the simulation study. Fig. 14 shows the average values of the misfit functions for each generation. The *S*-wave velocity profiles estimated from inversions by two proposed methods of forward modeling are shown in Figs 15 and 16. The standard deviations of inverted models using effective phase velocities are much higher than those using SPAC coefficients. The final *S*-wave velocity model by an inversion using effective phase velocities is poorly resolved. It is considered that this failure is caused by the discrepancies in the observed phase velocities below 4 Hz. Although the inversion using SPAC coefficients is also effected on the misfit below 4 Hz, the *S*-wave velocity consistent with logging data can be inverted.

Then, we considered giving a constraint in the inversion using effective phase velocities to improve the *S*-wave velocity estimation. Because the discrepancies of observed phase velocities below 4 Hz are considerably related with an infinite half-space of inverted *S*-wave velocity, we constrained the velocity of an infinite half-space to 700 m s^{-1} and the depth to 50 m as prior information in an inversion. Fig. 17 shows the result of the inversion by effective phase velocities when prior information is introduced. It can be seen that the *S*-wave velocity structure is better resolved. From this result, we suggest the objective function using SPAC coefficients (eq. 12)

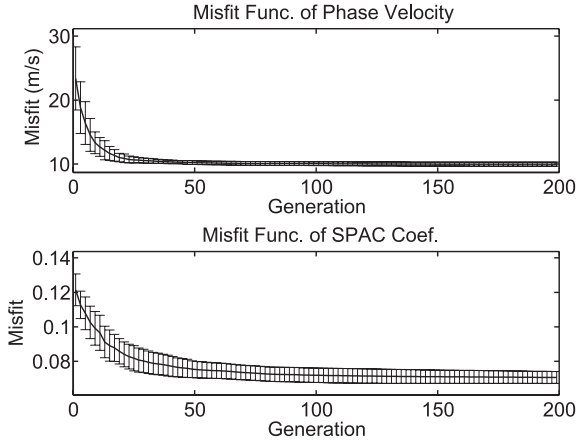

Figure 14. The average of the misfit functions in each generation for field data. The error bars shows the standard deviations.

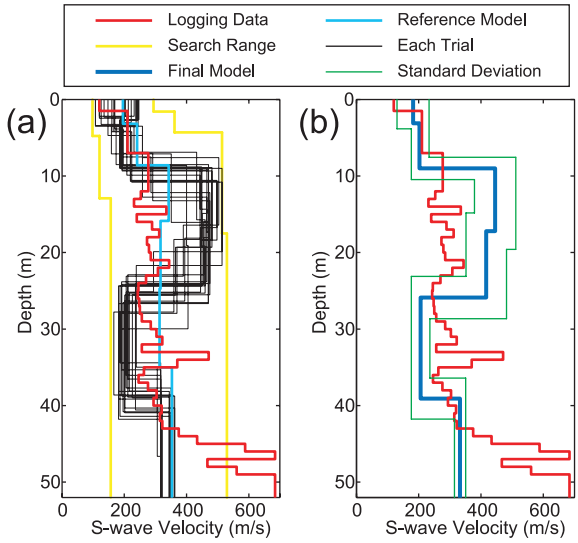

Figure 15. Results of inversions using effective phase velocities. (a) Logging data (red), reference model constructed by eqs (14) and (15) (cyan), inverted model for each trial (black) and the search range for the GA inversion (yellow). (b) Final inverted model obtained by averaging the *S*-wave velocities and thicknesses for each layer over 20 trials (blue) and their standard deviations (green).

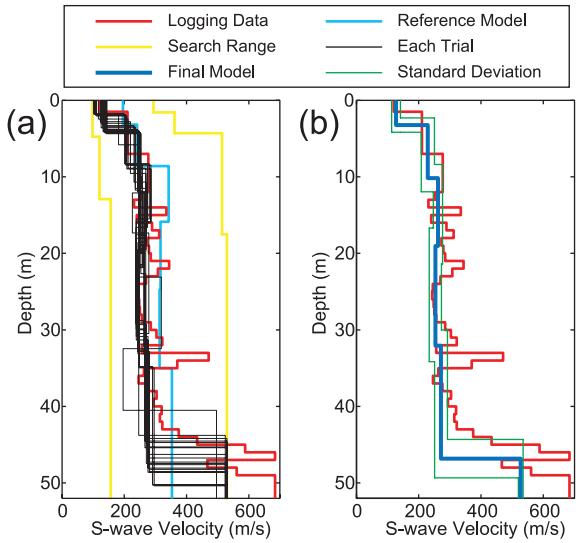

Figure 16. Results of inversions using SPAC coefficients. (a) Logging data (red), reference model constructed by eqs (14) and (15) (cyan), inverted models for each trial (black) and the search range for the GA inversion (yellow). (b) Final inverted model (blue) obtained by averaging the *S*-wave velocities and thicknesses for each layer over 20 trials and their standard deviations (green).

is robust than that using effective phase velocities (eq. 10) in the point that the former can give a better weighting for low frequencies when observed values have significant errors.

6 CONCLUSIONS

In this study, we proposed two multimode analyses in the SPAC method using amplitude response of surface waves. The use of amplitude response is superior in that there is no need to identify the observed modes, and therefore mode misidentification is avoided.

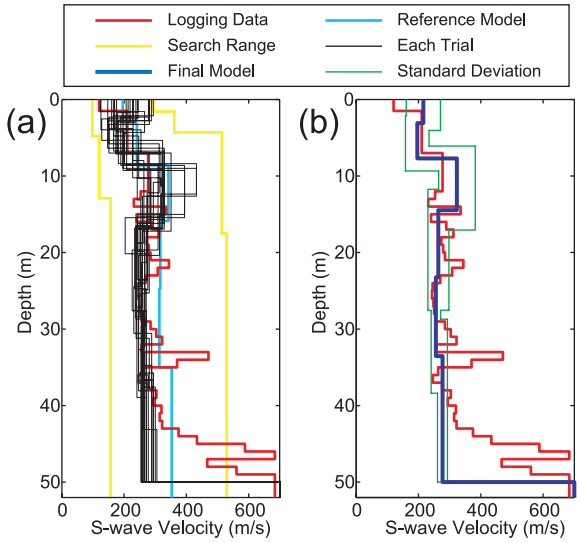

Figure 17. Results of inversions using effective phase velocities. The *S*-wave velocity and the depth of the infinite half-space were fixed at 700 m s^{-1} and 50 m, respectively. (a) Logging data (red), reference model constructed by eqs (14) and (15) (cyan), inverted models for each trial (black) and the search range for the GA inversion (yellow). (b) Final inverted model (blue) obtained by averaging the *S*-wave velocities and thicknesses for each layer of 20 trials and their standard deviations (green).

Practical application point of view, this point becomes important because it may solve an uncertainty problem by a lack of experimental knowledge of engineers. The first method is to calculate the theoretical effective phase velocities corresponding to the estimated ones by the ESPAC method. The second method is to fit SPAC coefficients directly. The latter approach is simpler than the former one.

To conduct quantitative verification, we simulated microtremors with predominant higher modes of surface waves. Although the estimated phase velocities from the ESPAC method were between theoretical phase velocities of fundamental mode and first higher mode at some frequencies, the theoretical effective phase velocities were consistent with the estimated ones. The observed SPAC coefficients were also consistent with the theoretical ones. These methods were included in the forward modeling of a GA inversion. The reversal layer of an *S*-wave velocity, which usually plays an important role in higher modes, was successfully inverted by both proposed methods.

In addition, we applied the proposed methods to field data in which higher modes were considered to be predominant from PS logging data. The *S*-wave velocity estimated by an inversion using SPAC coefficients is well-consistent with that from logging data. On the other hand, the inverted model using effective phase velocities was poorly resolved. Introduction of prior information about the infinite half-space layer, however, improved the result of the inversion.

The simulation study and field example demonstrated that results from our proposed methods are mostly in good agreement with the observed phase velocities and SPAC coefficients. However, these methods have to be applied carefully to an inversion analysis without any prior information. If the observed values have low quality for crucial *S*-wave velocities when applying the multimode analysis (e.g. below 4 Hz in Fig. 13), the inverted models may be trapped in the local minimum as in Fig. 15. Meanwhile, the *S*-wave velocity structure was successfully estimated by an inversion using SPAC coefficients without any constraints for the reference model. Because of this, we suggest that the multimode inversion using SPAC coefficients has a better weighting for low frequencies when observed values have significant errors and, therefore, it is more robust than an inversion using effective phase velocities. To verify the effectiveness of the proposed inversion methods, the observed microtremors need to be applied to various areas where borehole data are available for a quantitative evaluation.

ACKNOWLEDGMENTS

We thank Prof. Michael Asten at Monash University for useful comments. We are also grateful to two anonymous reviewers for helpful reviews of the manuscript. Authors acknowledge JST/JICA, SATREPS for supporting this research.

REFERENCES

Abbiss, C.P., 1983. Calculation of elasticities and settlements for longer periods of time and high strains from seismic measurements, *Geotechnique,* **33,** 397–405.

Aki, K., 1957. Space and time spectra of stationary stochastic waves, with special reference to microtremors, *Bull. Earthq. Res. Inst.,* **35,** 415–456.

Aki, K., 1965. A note on the use of microseisms in determining the shallow structures of the earth's crust, *Geophysics,* **30,** 665–666.

Asten, M.W., 1976. The use of microseisms in geophysical exploration, *PhD thesis*. Macquarie University.

Asten, M.W., 2001. The spatial auto-correlation method for phase velocity of microseisms—another method for characterisation of sedimentary overburden, in *Earthquake Codes in the Real World*, Australian Earthquake Engineering Soc., Proceedings of the 2001 Conference, Canberra, Paper 28.

Asten, M.W., 2006. On bias and noise in passive seismic data from finite circular array data processed using SPAC methods, *Geophysics,* **71,** V153–V162.

Asten, M.W., Dhu, T. & Lam, N., 2004. Optimised array design for microtremor array studies applied to site classification—Observations, results and future use, *Proceedings of the 13th Annual World Conference of Earthquake Engineering,* Vancouver, Paper 2903.

Asten, M.W., Lam, N., Gibson, G. & Wilson, J., 2002. Microtremor survey design optimised for application to site amplification and resonance modeling, in *Total Risk Management in the Privatised Era,* eds Griffith, M., Love, D., McDougall, P. & Butler, B., *Proceedings of Conference,* Australian Earthquake Engineering Soc., Adelaide, Paper 7.

Asten, M.W. & Robert, J., 2006. Analysis of ESG2006 blind-trial microtremor data using the MMSPAC method, Third International Symposium on the Effects of Surface Geology on Seismic Motion Grenoble, France, 2006 August 30–September 1, N01.

Bettig, B., Bard, P.Y., Scherbaum, F., Riepl, J., Cotton, F., Cornou, C. & Hatzfeld, D., 2001. Analysis of dense array noise measurements using the modified spatial auto-correlation method (SPAC): application to the Grenoble area, *Bollettino di Geofisica Teorica ed Applicata,* **42,** 281–304.

Bonnefoy-Claudet, S. *et al*. 2004. Simulation of seismic ambient noise. I. Results of H/V and array techniques on canonical models, in *Proc. 13th World Conf. on Earthquake Engineering,* Vancouver, Paper 2903.

Bonnefoy-Claudet, S., Cornou, C., Bard, P.-Y., Cotton, F., Moczo, P., Kristek, J. & Fäh, D., 2006a. H/V ratio: a tool for site effects evaluation. Results from 1-D noise simulations, *Geophys. J. Int.,* **167,** 827–837.

Bonnefoy-Claudet, S., Cotton, F. & Bard, P.-Y., 2006b. The nature of noise wavefield and its applications for site effects studies, A literature review, *Earth-Sci. Rev.,* **79,** 205–227.

Bouchon, M. & Aki, K., 1977. Discrete wavenumber representation of seismic wave fields, *Bull. seism. Soc. Am.,* **67,** 259–277.

Capon, J., 1969. High-resolution frequency-wavenumber spectrum analysis, *Proc. IEEE,* **57,** 1408–1418.

Chávez-García, F.J. & Luzón, F., 2005. On the correlation of seismic microtremors, *J. geophys. Res.,* **110,** B11313.

Cho, I., Tada, T. & Shinozaki, Y., 2004. A new method to determine phase velocities of Rayleigh waves from microseisms, *Geophysics,* **69,** 1535–1551.

Cho, I., Tada, T. & Shinozaki, Y., 2006. Centerless circular array method: inferring phase velocities of Rayleigh waves in broad wavelength ranges using microtremor records, *J. geophys. Res.,* **111,** B09315.

Cornou, C., Ohrnberger, M., Boore, D.M., Kudo, K. & Bard, P.-Y., 2006. Derivation of structural models from ambient vibration array recordings: results from an international blind test, *Proceedings of the Third International Symposium on the Effects of Surface Geology on Seismic Motion,* NBT, Grenoble, France.

Feng, S., Sugiyama, T. & Yamanaka, H., 2005. Effectiveness of multi-mode surface wave inversion in shallow engineering site investigations, *Expl. Geophys.,* **36,** 26–33.

Fotti, S., 2005. Surface wave testing for geotechnical characterization, in *Surface Waves in Geomechanics: Direct and Inverse Modelling for Soils and Rocks,* eds Lai, C.G. & Wilmanski, K., CISM Course and Lectures No.481, International Center for Mechanical Sciences, Springer, Vienna.

Goldberg, D.E., 1989. *Genetic Algorithms in Search, Optimization, and Machine Learning,* Addison-Wesley, Reading, MA.

Gucunski, N. & Woods, R.D., 1992. Numerical simulation of the SASW test, *Soil Dyn. Earthq. Eng.,* **11,** 213–227.

Harkrider, D.G., 1964. Surface waves in multilayered elastic media, Part 1. Rayleigh and Love waves from buried sources in a multilayered elastic half-space, *Bull. seism. Soc. Am.,* **54,** 627–679.

Harkrider, D.G., 1970. Surface waves in multilayered elastic media, Part 2. Higher mode spectra ratios from point sources in plane layered earth models, *Bull. seism. Soc. Am.,* **60,** 1937–1987.

Heisey, J.S., Stokoe, K.H., II, Hudson, W.R. & Meyer, A.H., 1982. Determination of in situ shear wave velocities from spectral analysis of surface waves, Res. Rep. 256–2, Ctr. for Transp. Res., Univ. of Texas, Austin, TX.

Kitsunezaki, C. *et al*. 1990. Estimation of P- and S-wave velocities in Deep Soil Deposits for Evaluating Ground Vibrations in Earthquake: Sizen-saigai-kagaku, 9–3, 1–17 (in Japanese).

Ling, S. & Okada, H., 1993. An extended use of the spatial autocorrelation method for the estimation of structure using microtremors, in *Proc. of the 89th SEGJ Conference,* 1993 October 12–14, Society of Exploration Geophysicists of Japan, Nagoya, Japan, pp. 44–48 (in Japanese).

Louie, J.N., 2001. Faster, better: shear-wave velocity to 100 meters depth from refraction microtremor arrays, *Bull. seism. Soc. Am.,* **91,** 347–364.

Ludwig, W.J., Nafe, J.E. & Drake, C.L., 1970. *Seismic Refraction in the Sea,* Vol. 4, part 1, Wiley-Interscience, p. 74.

Obuchi, T., Yamamoto, H., Sano, T. & Saito, T., 2004. Estimation of underground velocity structure based on both fundamental and higher modes, in *Proc. of the 111th SEGJ Conference,* Society of Exploration Geophysicists of Japan, pp. 25–28 (in Japanese with English abstract).

Ohori, M., Nobata, A. & Wakamatsu, K., 2002. A comparison of ESAC and FK methods of estimating phase velocity using arbitrarily-shaped microtremor arrays, *Bull. seism. Soc. Am.,* **92,** 2323–2332.

Okada, H., 2003. *The Microtremor Survey Method, Geophysical Monograph, No.12,* Society of Exploration Geophysicists, Tulsa, OK.

Okada, H., 2008. Present situation of the microtremor survey method and subject related to its practical application, *Butsuri-tansa,* **61,** 445–456 (in Japanese with English abstract).

O'Neill, A. & Matsuoka, T., 2005. Dominant higher surface modes and possible inversion pitfalls, *J. Eng. Environ. Geophys.,* **10,** 185–201.

Picozzi, M. & Albarello, D., 2007. Combining genetic and linearized algorithms for a two-step joint inversion of Rayleigh wave dispersion and H/V spectral ratio, *Geophys. J. Int.,* **169,** 189–200.

Richwalski, S. *et al*. 2007. Rayleigh wave dispersion curves form seismological and engineering-geotechnical methods: a comparison at the Bornheim test site (Germany), *J. Geophys. Eng.,* **4,** 349–361.

Roberts, J.C. & Asten, M.W., 2004. Resolving a velocity inversion at the geotechnical scale using the microtremor (passive seismic) survey method, *Expl. Geophys.,* **35,** 14–18.

Saito, M., 1988. DISPER80: a subroutine package for calculation of seismic normal-mode solution, in *Seismological Algorithm,* ed. Doorbos, D.J., Academic Press, San Diego, CA.

Socco, L.V., Foti, S. & Boiero, D., 2010. Surface-wave analysis for building near-surface velocity models—Established approaches and new perspectives, *Geophysics,* **75,** 75A83–75A102.

Suzuki, H. & Takahashi, T., 1999. S-wave velocity survey in Tukuba City by array microtremor measurements—Comparison with deep borehole data, *Proceeding of the 101th SEGJ Conference,* pp. 50–53 (in Japanese with English abstract).

Tokimatsu, K., 1997. Geotechnical site characterization using surface waves, in *Earthquake Geotechnical Engineering: Proceedings of IS-Tokyo'95, The First International Conference on Earthquake Geotechnical Engineering,* ed. Ishihara, K., A. A. Balkema, Rotterdam, pp. 1333–1368.

Tokimatsu, K., Tamura, S. & Kojima, H., 1992a. Effects of multiple modes on Rayleigh wave dispersion characteristics, *J. Geotech. Eng.,* ASCE, **118,** 1529–1543.

Tokimatsu, K., Tamura, S. & Kojima, H., 1992b. Use of short-period microtremors for Vs profiling, *J. Geotech. Eng.,* ASCE, **118**(10), 1544–1558.

Wathelet, M., Jongmans, D. & Ohrnberger, M., 2005. Direct inversion of spatial autocorrelation curves with the neighborhood algorithm, *Bull. seism. Soc. Am.,* **95,** 1787–1800.

Xia, J., Miller, R.D., Park, C.B. & Tian, G., 2003. Inversion of high frequency surface waves with fundamental and higher modes, *J. appl. Geophys.,* **52,** 45–57.

Yamanaka, H. & Ishida, H., 1996. Application of genetic algorithms to an inversion of surface-wave dispersion data, *Bull. seism. Soc. Am.,* **86,** 436–444.

Yokoi, T., 2010. New formulas derived from seismic interferometry to simulate phase velocity estimates from correlation methods using microtremor, *Geophysics,* **75,** SA71–SA83.

Zhang, S.X. & Chan, L.S., 2003. Possible effects of misidentified mode number on Rayleigh wave inversion, *J. appl. Geophys.,* **53,** 17–29.

APPENDIX

Here, we discuss how the distance between receivers influences to the theoretical calculation of effective phase velocities by using a simulated velocity structure (Fig. 3). Effective phase velocities from eq. (9) using a geometry of observation array and ones for $r = 7.21$,

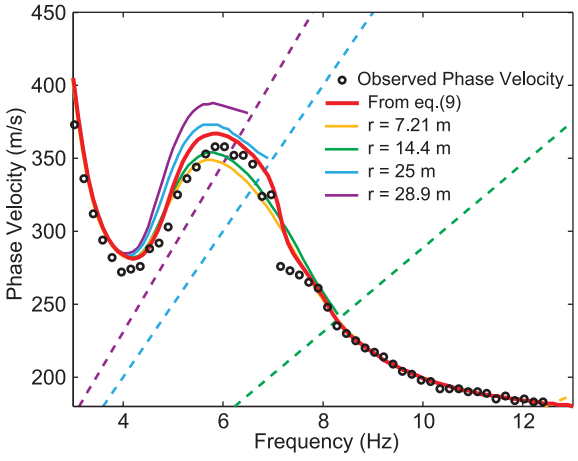

Figure A1. Effects on the theoretical calculation of effective phase velocities depending on the distance between receivers using simulated data. Observed phase velocities (black circles), theoretical phase velocities from eq. (9) and ones from eq. (8) for $r = 7.21$, 14.4, 25 and 28.9 m. Dashed lines show the limit of the high frequency caused by the spatial aliasing.

14.4, 25 and 28.9 m from eq. (8) are shown in Fig. A1. It can be seen that effective phase velocities from eq. (8) have some differences associated with the receiver interval. The frequency ranges where effective phase velocities can be calculated from eq. (8) are restricted by the spatial aliasing depending on the distance (dashed lines in Fig. A1).

In the calculation of effective phase velocities from eq. (9), however, there is no effect on the spatial aliasing at more than 20 Hz in addition to an agreement with observed values. This advantage would be important in an inversion because theoretical phase velocities have to be completely covered with the frequency range where phase velocities are estimated.